



Two-phase versus two-stage versus multi-phase lithiation kinetics in silicon

Zhiwei Cui, Feng Gao, and Jianmin Qu

Citation: [Applied Physics Letters](#) **103**, 143901 (2013); doi: 10.1063/1.4824064

View online: <http://dx.doi.org/10.1063/1.4824064>

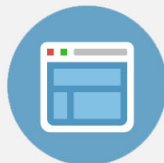
View Table of Contents: <http://scitation.aip.org/content/aip/journal/apl/103/14?ver=pdfcov>

Published by the [AIP Publishing](#)



Re-register for Table of Content Alerts

Create a profile.



Sign up today!



Two-phase versus two-stage versus multi-phase lithiation kinetics in silicon

Zhiwei Cui,¹ Feng Gao,¹ and Jianmin Qu^{1,2,a)}

¹Department of Civil and Environmental Engineering, Northwestern University, Evanston, Illinois 60208, USA

²Department of Mechanical Engineering, Northwestern University, Evanston, Illinois 60208, USA

(Received 16 August 2013; accepted 18 September 2013; published online 1 October 2013)

We classify the lithiation process into three types, namely, two-phase, two-stage, and multi-phase lithiation. We found that under a given charging rate, smaller electrochemical Biot number of β will likely to result in two-phase lithiation, while larger β may lead to multi-phase lithiation. For the film anode, intermediate β , or intermediate charging rate, will yield two-stage lithiation, and the Li concentration during the first stage of the lithiation is determined by the relationship between β and the charging rate (or more precisely the Li flux supplied to the Si/Li_xSi phase interface). Such two-stage lithiation does not occur in the particle or fiber anode. © 2013 AIP Publishing LLC.

[<http://dx.doi.org/10.1063/1.4824064>]

Lithium (Li) ion batteries have gained tremendous attention in recent years.^{1–4} Major effort has been invested in improving the storage capabilities of anode and cathode. Among all the candidate anode materials, silicon (Si) has the highest known theoretical charge capacity (>3500 mAh/g).^{5,6} However, crystalline Si (*c*-Si) anode may exhibit greater than 300% volumetric expansion after fully charged. Such large volumetric expansion generates significant mechanical stress, leading to fracture of the electrode.^{7,8} To overcome this failure mode, extensive effort has been devoted to understand the underline mechanisms of Li insertion into Si.^{9,10}

Based on experimental observations, the authors^{11,12} have developed a lithiation model that accounts for the interfacial chemical interactions between Li and Si by introducing an electrochemical Biot number $\beta = k_f^e V_m h_0 / D_0$, where k_f^e is the rate of chemical reaction at the Si/Li_xSi interface, D_0 is the rate of bulk diffusion of Li in Li_xSi, V_m is the molar volume of Si, and h_0 is a characteristic length of the anode. Clearly, β characterizes the ratio between the rate of interfacial chemical reaction and the rate of Li diffusion in Si.^{11,12} The model predicts that first intercalation of Li into *c*-Si will occur in a *two-phase* fashion, in which the unlithiated (*c*-Si) phase is separated from the fully lithiated (*a*-Li_{3.75}Si alloy) phase by a rather sharp interface that moves towards the unlithiated *c*-Si during the first lithiation process. In other words, the concentration of Li is $c = 1$ (equivalent to Li_{3.75}Si) in the lithiated phase and $c = 0$ in the unlithiated phase. Such a two-phase lithiation phenomenon has been observed experimentally by several research groups, e.g., Refs. 13–15.

Recently, TEM observations of an *a*-Si film seem to indicate that the lithiation kinetics in the *a*-Si film are different from that observed the *c*-Si film in that the lithiated phase is not fully saturated with Li.¹⁵ Instead, the Li concentration in the lithiated phase remains a constant $c = c_1 < 1$, and the phase interface moves towards the *a*-Si phase until the entire *a*-Si film is partially lithiated with Li concentration of $c = c_1 < 1$. After that, further lithiation causes Li

concentration in the partially lithiated phase to increase uniformly until full saturation, i.e., from $c = c_1$ to $c = 1$. We will call such kinetic process *two-stage* lithiation in order to distinguish it from the *two-phase* lithiation discussed in the previous paragraph. Such distinction is only semantic for the convenience of later discussions. In essence, the above defined two-stage lithiation becomes the two-phase lithiation when $c_1 \rightarrow 1$.

To understand the underline mechanism for the different types of kinetic processes, we first consider a Si (*a*-Si or *c*-Si) film with thickness h_0 . Assume that one surface of the Si film is attached to a rigid substrate at $\bar{X} = 0$ and a uniform flux of Li is prescribed on the other surface of the Si film at $\bar{X} = 1$ through the linearized Butler-Volmer equation,¹⁰ where \bar{X} is the dimensionless Lagrangian coordinate. For simplicity, all materials are assumed isotropic. Under these assumptions, the lithiation problem considered here is one-dimensional. By following the framework developed in Refs. 10 and 12, the governing equations for this one-dimensional problem can be written in terms of the dimensionless variables as

$$E_{11}^e = \frac{-2\nu}{1-\nu} E_{22}^e, \quad \text{for } \bar{S}(\bar{t}) < \bar{X} < 1, \quad (1)$$

$$\frac{1}{\lambda_p} \frac{\partial \lambda_p}{\partial \bar{t}} = -\text{sgn}(\sigma_{22}) \bar{d}_0 \left(\frac{\sigma_{eff}}{\sigma_f} - 1 \right)^m \text{H} \left(\frac{\sigma_{eff}}{\sigma_f} - 1 \right),$$

$$\text{for } \bar{S}(\bar{t}) < \bar{X} < 1, \quad (2)$$

$$\frac{\partial c}{\partial \bar{t}} + \frac{\partial \bar{J}}{\partial \bar{X}} = 0, \quad \bar{J} = -\frac{1}{F_{11}^2 R_g T} c \frac{\partial \mu}{\partial \bar{X}} \quad \text{for } \bar{S}(\bar{t}) < \bar{X} < 1, \quad (3)$$

where $\bar{X} = X_1/h_0$, $\bar{D} = D/D_0$, $\bar{t} = D_0 t/h_0^2$, $\bar{u} = u/h_0$, $\bar{S} = S/h_0$, and \bar{d}_0 are non-dimensional coordinate, diffusivity, time, displacement and the location of Si/Li_xSi interface, and characteristic strain rate for plastic flow in Li_xSi, respectively. In addition, D_0 is the diffusivity of Li in *a*-Si, E_{11}^e and E_{22}^e are the elastic strains along X_1 - and X_2 -axis, ν is the Poisson's ratio of pure Si, λ_p is the plastic stretch, σ_{22} is the Cauchy stress along the X_2 -axis, and σ_{eff} and σ_f are the

^{a)} Author to whom correspondence should be addressed. Electronic mail: j-qu@northwestern.edu. Telephone: 847-467-4528

effective stress and yield stress, respectively. The boundary conditions at the interfaces are expressed as follows:

$$\bar{J} = \bar{J}_0(1 - c), \quad \text{for } \bar{X} = 1, \quad (4)$$

$$\bar{J} = -x_0\beta\bar{R}_s(c)/x_{\max}, \quad \text{for } \bar{X} = \bar{S}^+(\bar{t}), \quad (5)$$

$$\bar{V}(\bar{t}) \equiv d\bar{S}(\bar{t})/d\bar{t} = -\beta\bar{R}_s(c), \quad \text{for } \bar{X} = \bar{S}^-(\bar{t}), \quad (6)$$

where $x_0 \approx 0.2$ is the minimum value to form an amorphous Li_{x_0}Si alloy, $x_{\max} = 3.75$ represents the saturation concentration of Li in Li_xSi , $\bar{R}_s(c)$ is the effective chemical reaction rate, and k_f^e is the effective forward reaction rate constant for the Li-Si reaction. Note that $\beta = k_f^e V_m h_0 / D_0$ determines the nature of the diffusion/reaction kinetics at the Si/ Li_xSi interface.^{11,12}

As a numerical example, we take $\bar{J}_0 = 0.1$ and $\beta = 0.6$. Material properties and other parameters are the same as used in Refs. 12 and 16. Shown in Figure 1(a) is the Li concentration profile $c(\bar{X}, \bar{t})$ at different charging times. Clearly, the lithiation process consists of two stages. In the first stage, a sharp interface between the Si and the $a\text{-Li}_x\text{Si}$ alloy is formed, and moves towards the Si phase. During this stage, the distribution of Li in the $a\text{-Li}_x\text{Si}$ phase is rather uniform and remains roughly the same value $c_1 \approx 0.6$ until the entire Si film has been partially lithiated. The second stage starts when the entire Si film has been partially lithiated. Further lithiation causes the Li concentration to increase almost uniformly throughout the partially lithiated film until Li reaches its saturation. During the second stage, the charging proceeds rather slowly because of the near zero Li concentration gradient. Such a two-stage phenomenon has been observed recently in thin $a\text{-Si}$ films by *in-situ* TEM.¹⁵ As another example, we computed the distribution of Li concentration for $\bar{J}_0 = 0.1$ and $\beta = 50$, see Figure 1(b). Clearly, this case does not exhibit the two-stage phenomenon in that the Li concentration in the partially lithiated phase continues to increase as the phase interface moves forward. Furthermore, unlike in the two-phase case, there are multiple Li concentrations in the anode at any given time during the lithiation

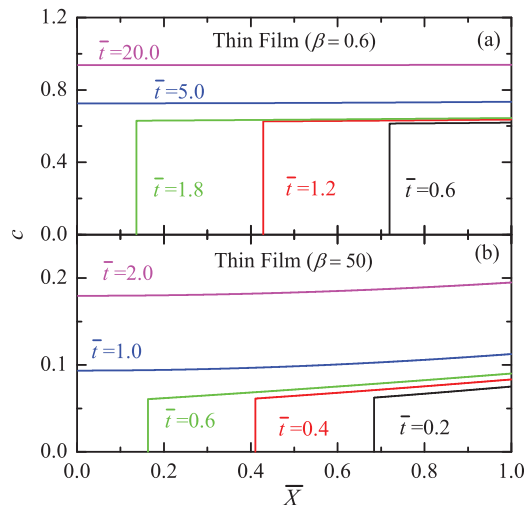


FIG. 1. Li concentration profiles at different times. (a) $\beta = 0.6$ and (b) $\beta = 50$.

process. For these reasons, we will call this phenomenon *multi-phase* lithiation to distinguish it from the *two-phase* and *two-stage* lithiations discussed earlier.

We note that the kinetics of the lithiation is controlled by three rates, namely, the charging rate \bar{J}_0 , the diffusion rate D_0 , and the chemical reaction rate k_f^e . The competition between the latter two rates can be represented by the non-dimensional Biot number β . As pointed out in Refs. 11 and 12, under a given charging rate \bar{J}_0 , the overall lithiation kinetics is controlled by chemical reaction when $\beta \ll 1$ and by diffusion when $\beta \gg 1$. To understand how the overall kinetic process is affected by the Biot number β , we computed $c(\bar{X}, \bar{t})$ in an $a\text{-Si}$ film with different values of β . We are particularly interested in $c(0, \bar{t}_1)$ and $c(1, \bar{t}_1)$ versus β , where \bar{t}_1 is the time when the Li arrives at the substrate/anode interface. By definition, $c(0, \bar{t}_1)$ and $c(1, \bar{t}_1)$ are the Li concentrations at the anode/electrolyte interface and the substrate/anode interface, respectively, when the moving front of Li arrives at substrate/anode interface.

For visual convenience, we define $\bar{c}(\bar{t}) = c(1, \bar{t})/c(0, \bar{t}_1)$ and plotted it in Figure 2(a) as a function of \bar{t}/\bar{t}_1 . If $\bar{c}(\bar{t}) \approx 1$, one can say that the distribution of Li across the film thickness is rather uniform at all times, which would be the case for either the two-phase or the two-stage process. An increasing $\bar{c}(\bar{t})$ means that the Li concentration at the anode/electrolyte interface increases with time, which corresponds to the multi-phase lithiation phenomenon discussed earlier. It is seen from this plot that for large $\beta \gg 1$, the Li concentration at the anode/electrolyte interface ($\bar{X} = 1$) quickly reaches an initial value, then continues to increase as the phase interface moves toward the anode/substrate interface ($\bar{X} = 0$), indicating a multi-phase process. For example, in the case of $\beta = 100$, by the time the phase interface reaches the anode/substrate interface, the Li concentration at the anode/electrolyte interface has more than 50% of the value at the substrate/anode interface. On the other hand, for small $\beta \ll 1$, the Li concentration at the anode/electrolyte interface ($\bar{X} = 1$) also quickly reaches an initial value and then remains at this value until the phase interface reaches the

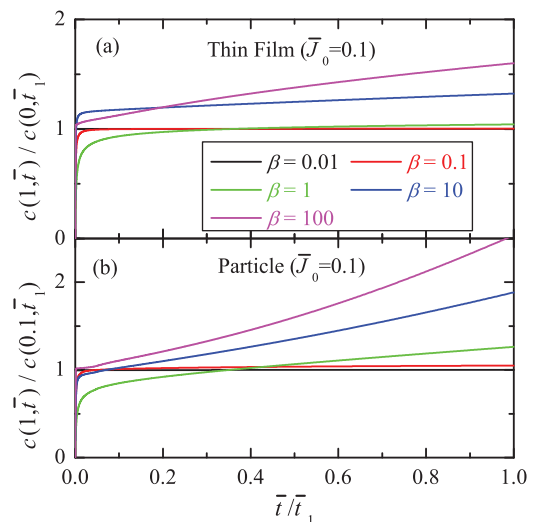


FIG. 2. (a) $\bar{c}(\bar{t}) = c(1, \bar{t})/c(0, \bar{t}_1)$ as a function of normalized time \bar{t}/\bar{t}_1 for a Si film anode and (b) $\bar{c}(\bar{t}) = c(1, \bar{t})/c(0.1, \bar{t}_1)$ as a function of normalized time \bar{t}/\bar{t}_1 for a Si particle anode.

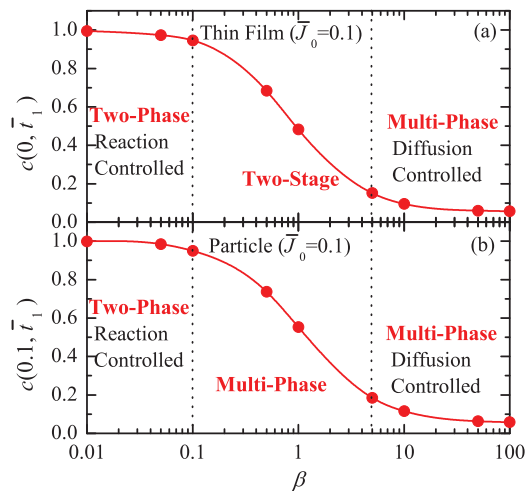


FIG. 3. (a) $c(0, \bar{t}_1)$ versus β for a Si film anode and (b) $c(0.1, \bar{t}_1)$ versus β for a Si particle anode.

anode/substrate interface ($\bar{X} = 0$), indicating a uniform distribution of Li $c(\bar{X}, \bar{t}) \approx c(0, \bar{t}_1)$ for $\bar{t} \in (0, \bar{t}_1]$.

To investigate whether the process is two-phase or two-stage, we plot how $c(0, \bar{t}_1)$ varies with β in Figure 3(a). We see that $c(0, \bar{t}_1) \approx 1$ for $\beta < 0.1$. For this range of β , we also learned from Figure 2(a) that $c(\bar{X}, \bar{t}) \approx c(0, \bar{t}_1)$ for $\bar{t} \in (0, \bar{t}_1]$. These are the characteristics of the *two-phase* lithiation discussed early, i.e., lithiation proceeds with a moving sharp interface dividing the unlithiated Si phase and an almost fully lithiated $\text{Li}_{3.75}\text{Si}$ phase. For $0.1 < \beta < 5$, we see that $0 < c(0, \bar{t}_1) < 1$. For this range of β , we learned also from Figure 2(a) that $c(\bar{X}, \bar{t}) \approx c(0, \bar{t}_1)$ for $\bar{t} \in (0, \bar{t}_1]$. These are the characteristics of the *two-stage* lithiation discussed early, i.e., lithiation proceeds with a moving sharp interface dividing the unlithiated Si phase and a partially lithiated Li_xSi phase with $x < 3.75$. For $\beta > 5$, we see that $c(0, \bar{t}_1) \approx 0$. For this range of β , we learned also from Figure 2(a) that $c(\bar{X}, \bar{t})$ is not uniform for $\bar{t} \in (0, \bar{t}_1]$, and there is a significant spatial gradient of $c(\bar{X}, \bar{t})$. Therefore, it is the case of *multi-phase* lithiation.

To summarize the foregoing discussions, we demonstrated that the characteristics of lithiation kinetics are results of the interplay between the charging rate \bar{J}_0 and the electrochemical Biot number β . Under a given charging rate \bar{J}_0 , the lithiation proceeds in a two-phase fashion for very small β , in a two-stage fashion for intermediate β , and in a multi-phase fashion for very large β . Moreover, the values of β that distinguish these three types of kinetics processes also depend on the charging rate \bar{J}_0 , and the transition from one type to another occurs gradually. The correlation between \bar{J}_0 and β can be found in Figure 4. Clearly, large \bar{J}_0 has the tendency to become more two-phase process while small \bar{J}_0 is apt to multi-phase process.

We further note that there is no fundamental difference between the first lithiation of a *c*-Si and an *a*-Si, except that the interfacial chemical reaction rate is much slower between *c*-Si and Li than between *a*-Si and Li, since it is much more difficult for the Li to break the *c*-Si bonds than the *a*-Si bonds. Under the boundary condition of $\bar{J}_0 = 0.1$, our model predictions, see Figure 1(a), show that $\beta \approx 0.6$ in order for $c_1 \approx 0.6$, which is the value measured in Ref. 15. Since the

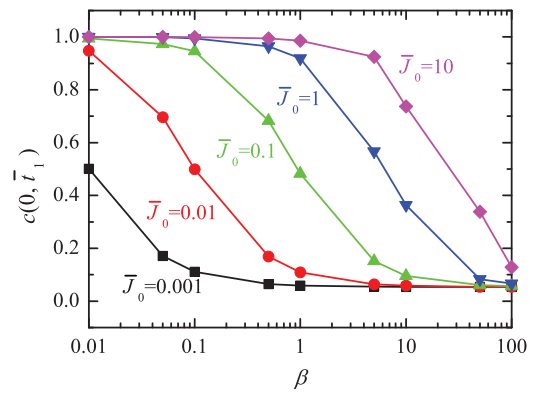


FIG. 4. $c(0, \bar{t}_1)$ versus β for different \bar{J}_0 in a Si film anode.

first lithiation of a *c*-Si film is observed to be two-phase,¹⁷ one may conclude from Figure 3(a) that $\beta < 0.1$ for a *c*-Si film. In other words, the ratio of the chemical reaction rate of lithiation into *a*-Si to that of lithiation into *c*-Si should be greater than 6.

Now we turn our attention to the first lithiation of an *a*-Si particle of radius R_0 . Since this case had been considered in our previous work,¹² we will reproduce only results that are relevant to the discussions here. Similarly to the Si film anode case, $\bar{c}(\bar{t}) = c(1, \bar{t})/c(0.1, \bar{t}_1)$ as a function of normalized time \bar{t}/\bar{t}_1 for a Si particle anode is plotted in Figure 2(b) and the corresponding $c(0.1, \bar{t}_1)$ versus β curve is plotted in Figure 3(b). Note that the \bar{t}_1 here is taken to be the time when the Si/ Li_xSi interface is at very close to the center of the particle, i.e., at $\bar{R} = 0.1$, to avoid dealing with the singular behavior of the solution at $\bar{R} = 0$. We note that excluding the core $\bar{R} = 0.1$ removes only 0.1% of the total volume of the particle. Following the discussions on the film case, one can see that $\beta \leq 0.1$ leads to the two-phase lithiation and other β leads to the multi-phase lithiation. Careful parametric studies show that there is no two-stage lithiation for the case of particle anode.

In summary, we classify the lithiation process into three types, namely, two-phase, two-stage, and multi-phase lithiation. In the case of two-phase lithiation, the anode has a pure Si phase and a fully lithiated $\text{Li}_{x_{\max}}\text{Si}$ phase at all times of the charging process. In the case of the two-stage lithiation in the film anode, the anode has a pure Si phase and a partially lithiated phase Li_{x_0}Si , where $x_0 < x_{\max}$ remains a constant during the first stage of the lithiation, which is defined as the duration from the start of the lithiation to the time when the Li front arrives at the substrate/anode interface. In the second stage, the Li concentration increases almost uniformly across the partially lithiated phase. Typical features of a two-stage lithiation are shown in Figure 1(a). In the case of multi-phase lithiation, the anode contains “multiple phases” at all times during the lithiation in that the Li concentration in the partially lithiated region is not uniform, therefore multi-phase. Figure 1(b) shows the features of the multi-phase lithiation.

We found that under a given charging rate, small β will likely to result in two-phase lithiation, while large β may lead to multi-phase lithiation. Equivalently, for a given β , higher charging rate is likely to induce two-phase lithiation, while lower charging rate may result in multi-phase lithiation. For the film anode, intermediate β , or intermediate charging rate,

will yield two-stage lithiation, and the Li concentration during the first stage of the lithiation is determined by the relationship between β and the charging rate (or more precisely the Li flux supplied to the Si/Li_xSi phase interface). Such two-stage lithiation phenomenon does not occur in the particle or fiber anode. The reason is that the area of the interface between the unlithiated and partially lithiated regions keeps shrinking as the interface propagates toward the center of the particle/fiber due to the spherical geometry; thus, the Li flux at the Si/Li_xSi interface in such non-planar geometry cannot remain constant as the phase interface propagates. This makes it impossible to maintain a constant c_1 as the phase interface moves towards the center of the particle/fiber.

In closing, we want to point out that in order to understand the basic mechanisms of the competition between bulk diffusion and interfacial chemical reaction, the dependence of materials properties (including the interfacial chemical reaction rate) on the stress (or on Li concentration) was not considered in this paper. Such dependence, as well as other factors such as self-limiting lithiation¹⁸ may also play a role in determining the lithiation characteristics.

This work was supported by NSF through No. CMMI-1200075.

- ¹C. K. Chan, H. L. Peng, G. Liu, K. McIlwrath, X. F. Zhang, R. A. Huggins, and Y. Cui, *Nat. Nanotechnol.* **3**, 31 (2008).
- ²L. F. Cui, R. Ruffo, C. K. Chan, H. L. Peng, and Y. Cui, *Nano Lett.* **9**, 491 (2009).
- ³X. H. Liu, L. Q. Zhang, L. Zhong, Y. Liu, H. Zheng, J. W. Wang, J. H. Cho, S. A. Dayeh, S. T. Picraux, J. P. Sullivan, *et al.*, *Nano Lett.* **11**, 2251 (2011).
- ⁴B. Scrosati and J. Garche, *J. Power Sources* **195**, 2419 (2010).
- ⁵U. Kasavajjula, C. S. Wang, and A. J. Appleby, *J. Power Sources* **163**, 1003 (2007).
- ⁶K. Kang, H. S. Lee, D. W. Han, G. S. Kim, D. Lee, G. Lee, Y. M. Kang, and M. H. Jo, *Appl. Phys. Lett.* **96**, 053110 (2010).
- ⁷V. L. Chevrier and J. R. Dahn, *J. Electrochem. Soc.* **156**, A454 (2009).
- ⁸S. Bourderau, T. Brousse, and D. M. Schleich, *J. Power Sources* **81**, 233 (1999).
- ⁹Y. F. Gao, M. Cho, and M. Zhou, *J. Mech. Phys. Solids* **61**, 579 (2013).
- ¹⁰Z. W. Cui, F. Gao, and J. M. Qu, *J. Mech. Phys. Solids* **60**, 1280 (2012).
- ¹¹Z. Cui, F. Gao, and J. Qu, *Acta Mech. Sinica* **28**, 1049 (2012).
- ¹²Z. Cui, F. Gao, and J. Qu, *J. Mech. Phys. Solids* **61**, 293 (2013).
- ¹³M. T. McDowell, S. W. Lee, J. T. Harris, B. A. Korgel, C. Wang, W. D. Nix, and Y. Cui, *Nano Lett.* **13**, 758 (2013).
- ¹⁴M. T. McDowell, I. Ryu, S. W. Lee, C. M. Wang, W. D. Nix, and Y. Cui, *Adv. Mater.* **24**, 6034 (2012).
- ¹⁵J. W. Wang, Y. He, F. Fan, X. H. Liu, S. Xia, Y. Liu, C. T. Harris, H. Li, J. Y. Huang, S. X. Mao, *et al.*, *Nano Lett.* **13**, 709 (2013).
- ¹⁶Z. W. Cui, F. Gao, Z. H. Cui, and J. M. Qu, *J. Power Sources* **207**, 150 (2012).
- ¹⁷M. J. Chon, V. A. Sethuraman, A. McCormick, V. Srinivasan, and P. R. Guduru, *Phys. Rev. Lett.* **107**, 045503 (2011).
- ¹⁸X. H. Liu, F. F. Fan, H. Yang, S. L. Zhang, J. Y. Huang, and T. Zhu, *ACS Nano* **7**, 1495 (2013).